ISLAMIC AZAD UNIVERSITY
MARVDASHT BRANCH

Journal of Building Information Modeling
Spring 2025. Vol 1. Issue 1

https://sanad.iau.ir/journal/bim

ORIGINAL RESEARCH PAPER

Accuracy Investigation of Linear Dynamic Analysis for Estimating Local Deformation Demands of Regular MDOF Systems Using SDOF Inelastic Displacement Ratio

Mojtaba Zare: MSc, Department of Civil Engineering, Shi.C, Islamic Azad University, Shiraz, Iran
Ashkan Sharifi*: Assistant Professor, Department of Civil Engineering, Shi.C., Islamic Azad University, Shiraz, Iran

A R T I C L E I N F O

Received:2025/02/28
Accepted:2025/06/08
PP: 1-18

Use your device to scan and read the article online

Keywords: *Linear Dynamic Analysis, Local Deformation Demands, MDOF Systems, SDOF Inelastic Displacement Ratio.*

Abstract

The displacement coefficient method and the inelastic displacement ratio have been the topic of several investigations over the last two decades. Although the vast majority of the previous investigations are related to the single degree of freedom (SDOF) systems, some seismic design and retrofit codes have generalized the results of these investigations for estimating the local responses of structures via the linear elastic dynamic analyses. The question arises whether the use of SDOF inelastic displacement ratios is sufficient for estimating the local responses of multi-degrees of freedom (MDOF) systems? The objectives of this paper are: (i) to review previous investigations on the inelastic displacement ratio for identifying the important factors that affecting the inelastic displacement ratio, and (ii) to investigate the accuracy of linear dynamic analysis for estimating local deformation demands of regular MDOF systems using SDOF inelastic displacement ratio. Results indicate that although the inelastic displacement ratio obtained from SDOF systems provides an acceptable estimation of the global response of MDOF systems, it is not suitable for estimating the local responses of the MDOF systems.

Citation: Zare, M., & Sharifi, A. (2025). **Accuracy Investigation of Linear Dynamic Analysis for Estimating Local Deformation Demands of Regular MDOF Systems Using SDOF Inelastic Displacement Ratio**. *Journal of Building Information Modeling*, 1(1), 1-18.

* Corresponding author: Ashkan Sharifi, Email: ashkan.sharifi@iau.ac.ir

INTRODUCTION

Estimating seismic deformation demands of structures has acquired renewed importance as a result of the tendency of the profession to move toward performance-based seismic design. Although the nonlinear dynamic analysis is the most accurate method for estimating the seismic deformation demands of a structure, it is not practical for day-to-day design due to the high computational intensity and the difficulty of interpreting its results. To avoid these difficulties, several approximate methods have been developed by researchers for estimating seismic deformation demands. One of the simplest approximate methods is to use the linear dynamic analysis results that are magnified by a displacement modification factor. In the other word, the maximum deformation of an inelastic system is approximated as a product of the maximum deformation of an elastic system with the same lateral stiffness and the same damping coefficient as the inelastic system times a displacement modification factor. This approach which is accepted by ASCE/SEI 41-13 (ASCE, 2014), FEMA 356 (ASCE, 2000), FEMA 440 (ATC, 2005) and many other building codes has been referred to as the coefficient method. The displacement modification factor which is defined as the ratio of the maximum inelastic to the maximum elastic displacement of a single degree of freedom (SDOF) system has been referred to as inelastic displacement ratio.

Several investigations have been conducted to develop the relationships between the peak deformations of inelastic and corresponding linear elastic systems and the influences of many parameters such as period of vibration, level of ductility demand, strength ratio, post-yield stiffness, site conditions, earthquake magnitude, and distance to source have been evaluated and discussed (Veletsos and Newmark, 1960; Veletsos, Newmark and Chelapati, 1965; Newmark and Hall, 1982; Miranda, 2000, 2001; Chopra and Chintanapakdee, 2001, 2004; Riddell, Garcia and Garces, 2002; Miranda and Ruiz-García, 2002; Ruiz-García and Miranda, 2003, 2004, 2006, 2007; Akkar and Miranda, 2005; Chenouda and Ayoub, 2008; Mollaioli and Bruno, 2008; Hatzigeorgiou and Beskos, 2009; Ruiz-García, 2011; Durucan and Dicleli, 2015; Durucan and Durucan, 2016). The vast majority of these investigations are related to the SDOF systems. This is due to the fact that the main goal of most of these investigations was to develop a relationship for estimating the target displacement (roof displacement demand) of structures which is used in the nonlinear equivalent static analysis procedures. In the other word, the coefficient method has been only used to estimate the global response (roof displacement) of the structures and the local responses such as inter-story drift and plastic hinge rotations have been estimated from the nonlinear equivalent static analysis. However, some seismic design and retrofit codes (ASCE, 2000, 2014) have generalized these relationships for estimating the local responses of structures via the linear elastic dynamic analyses (response spectrum or response history). The question arises whether the use of SDOF inelastic displacement ratios is sufficient for estimating the local responses of multi-degrees of freedom (MDOF) systems?

The above question arises from two issues. First, although the contribution of higher modes to the roof displacement is usually weak, their contribution to the local responses could be very important. Secondly, SDOF systems are statistically determinate structures while MDOF systems are statistically indeterminate structures whose post-yield behavior is accompanied by the force re-distribution between their members. Thus, even if the inelastic displacement ratios obtained from SDOF systems provide a good estimation of the global response of MDOF systems, their use to estimate the local responses of the MDOF systems is questionable and should be investigated carefully. The main goal of this paper is to answer the above-mentioned question and this is a distinguishing feature of this research in comparison with the previous researchers. Another objective of this paper is to review previous investigations for categorizing their results based on the factors that may affect the inelastic displacement ratio.

Literature Review

The inelastic displacement ratio has been the topic of several investigations over the last two decades. The vast majority of these investigations are related to the SDOF systems. In the following, the conducted literature

review on factors that may affect the inelastic displacement ratio, C, is described.

Spectral regions and characteristic period

A response spectrum is the peak response of a series of simple oscillators of different natural periods, T, when subjected to a particular earthquake ground motion. The response spectrum may be plotted as a curve on tripartite logarithmic graph paper showing the variation of the peak spectral acceleration, displacement, and velocity of the oscillators as a function of vibration period and damping. The response spectrum is generally divided into three regions so-called acceleration-, velocity- and displacement-sensitive region. Characteristic period, T_c, divides the acceleration-sensitive spectral region from the velocity-sensitive region. The basis of the coefficient method returns to the investigations conducted by Veletsos and Newmark (Veletsos and Newmark, 1960) and Veletsos *et al.* (Veletsos, Newmark and Chelapati, 1965) in 1960s. Using SDOF systems subjected to simple pulses and to three earthquake ground motions, they observed that in the short and moderate period range, the inelastic displacements were significantly higher than their elastic counterparts while in the long period region (low frequency range) the maximum deformation of the inelastic and elastic systems was approximately the same. This observation gave rise to the well-known equal displacement rule for long period structures, which is the basis for estimating maximum deformations in specific spectral regions in most building codes. These investigations provided the basis for the well-known Newmark and Hall (Newmark and Hall, 1982) method to estimate inelastic response spectra from the elastic one. This method provides some relationships for C in different spectral regions. For velocity-sensitive and displacement-sensitive spectral regions (periods longer than T_c) the strength ratio, R, is approximately equal to the demand ductility, μ, which leads to $C \cong 1$ that corresponds to the equal displacement rule, which states that in this period range the maximum displacement of an inelastic system is equal to the maximum displacement of an elastic system with the same lateral stiffness and the same damping coefficient as the inelastic system. For acceleration sensitive regions, the absorbed energy is the same in the inelastic and the corresponding elastic systems at maximum deformation which referred to as equal energy Rule. But For very short periods, the strength ratio is equal to one, which leads to an inelastic displacement ratio equal to demand ductility and the whole base acceleration will be transmitted to the system mass (equal acceleration rule). Similar rules have been observed by many other researchers (Miranda, 2000; Chopra and Chintanapakdee, 2001, 2004; Riddell, Garcia and Garces, 2002; Ruiz-García and Miranda, 2003; Mollaioli and Bruno, 2008). Thus, proper recognizing of spectral regions is the important factor. Inelastic displacement ratios for different site class and ground motions (far-fault and near-fault) are similar over all spectral regions if the period scale is normalized relative to the T_c value (Chopra and Chintanapakdee, 2001, 2004; Ruiz-García and Miranda, 2003). Chopra and Chintanapakdee (Chopra and Chintanapakdee, 2001) concluded that If the design equations for C explicitly recognize the spectral regions (such as Newmark and Hall equation) then the same equations may be applicable to various classes of ground motions (far-fault and near-fault, firm soil and soft soil, smaller magnitude and larger magnitude earthquakes) as long as the appropriate divisions for spectral regions are used.

Velocity spectrum predominant period of the ground motion

Velocity spectrum predominant period of the ground motion, T_g, is defined as the period corresponding to the maximum ordinate in the relative velocity spectrum computed for an elastic SDOF system having 5% damping ratio. Response data for 118 ground motion records on soft soils demonstrated that T_g is an important factor and normalizing periods of vibration by T_g results in a better characterization (smaller dispersion) of deformation demands in structures built on soft soil (Ruiz-García and Miranda, 2006). For systems with periods of vibration smaller than about $0.75\ T_g$, inelastic displacement ratios are larger than unity and increase linearly with increase in displacement ductility ratio. However, for systems with periods of vibration close to T_g, inelastic displacement ratios are, on average, significantly smaller than unity. This means that, in this spectral region, the well-known equal displacement rule will

significantly overestimate lateral displacement demands of inelastic systems practically for any ground motion recorded on very soft soils. For systems with periods of vibration that are more than 1.5 times the T_g, the inelastic displacement ratios are, on average, close to one. With the exception of periods close to T_g, levels of dispersion of inelastic displacement ratios of soft soil sites are smaller than those of firm sites (Ruiz-García and Miranda, 2004, 2006).

Near-fault ground motions and pulse period

Horizontal ground motion components oriented normal to the fault strike recorded within the near-fault region of an earthquake at stations located toward the direction of the fault rupture are typically, but not always, characterized for having a noticeable large velocity pulse. This large velocity pulse is a result of forward-directivity effects that occur when the earthquake rupture moves towards the site at a velocity slightly less than the velocity of the shear waves and the direction of the fault slip is aligned with the site (Ruiz-García, 2011). The pulse period, T_p, is the period associated to the main pulse in the ground velocity time history. T_p is the most important near-fault ground motion characteristic that influences the shape and amplitude of the inelastic displacement ratio, which is particularly true for systems with T shorter than T_g. An investigation based on 40 forward-directivity near-fault ground motions showed that for systems with T smaller than about $0.85T_p$, inelastic displacement ratios are, on average, larger than one and its ordinates increases nonlinearly with increasing R. For systems with T between 0.85 and 2.0 times T_p, inelastic displacement ratios are, on average, significantly smaller than one. For systems with T that are more than $2.0T_p$, inelastic displacement ratios are, on average, close to unity. Moreover, forward-directivity near-fault ground motions with T_g shorter than $1.0\ s$ leads to a local amplification for systems with T near $0.5T_p$ (Ruiz-García, 2011).

From the review of the literature (Bray and Rodriguez-Marek, 2004; Ruiz-García, 2011), it can be found that there is a good correlation between T_p and T_g from a statistical point of view. In general, it was found that the scatter of inelastic displacement ratios for forward-directivity near-fault ground motions is smaller when the period of vibration is normalized with respect to T_g instead of T_p (Ruiz-García, 2011). Although the two components of most far-fault records are quite similar in their demands, the fault-normal component of near-fault ground motions usually imposes much larger deformation and strength demands compared to the fault-parallel component over a wide range of vibration periods. The velocity-sensitive spectral region for the fault-normal component of near-fault records is much narrower, and their acceleration-sensitive and displacement-sensitive regions are much wider, compared to far-fault motions. The narrower velocity-sensitive region of near-fault records is shifted to longer periods (Chopra and Chintanapakdee, 2001). In the acceleration-sensitive spectral region, the average C versus T plots for near-fault ground motions are systematically different than far-fault ground motions. However, if the period scale is normalized relative to the T_c value, they become very similar in all spectral regions (Chopra and Chintanapakdee, 2004).

Peak ground acceleration to peak ground velocity ratio

The ratio of peak ground acceleration to peak ground velocity, A_p/V_p, of ground motions have a significant effect on inelastic displacement ratio, particularly for systems with high ductility levels (Zhai et al., 2007; Yaghmaei-Sabegh, 2012; Durucan and Dicleli, 2015). This ratio is a function of the earthquake magnitude, distance to fault, faulting mechanism and site class. A more recent investigation based on 98 near-fault pulse-type and 306 far-fault ground motion records showed that for earthquakes with small A_p/V_p ratios, inelastic displacement ratios obtained using ground motions recorded on the same NEHRP site are significantly scattered for periods smaller than $2.0\ s$ and for large strength ratio R. Moreover, for smaller A_p/V_p ratios, the inelastic displacement ratios were observed to dramatically increase, particularly for periods smaller than $1.0\ s$, while for periods larger than $1.5\ s$, the effect of the A_p/V_p diminishes and inelastic displacement ratio approaches unity (Durucan and Dicleli, 2015). It should be noted that the smaller values for A_p/V_p are related to stronger ground motions.

Faulting mechanism, earthquake magnitude and distance to rupture

In summary, the fault type mechanism is observed to affect the variation of inelastic displacement ratio in the short period range (Durucan and Dicleli, 2015). The earthquake magnitude is found to affect the value of C for periods smaller than 1.0 s and for larger R values (Ruiz-García and Miranda, 2003; Durucan and Dicleli, 2015).

For periods of vibration longer than 1.0 s changes in earthquake magnitude do not affect inelastic displacement ratios (Miranda, 2000; Chopra and Chintanapakdee, 2001, 2004; Ruiz-García and Miranda, 2003, 2004, 2006). With the exception of very near-field sites that may be influenced by forward directivity effects, inelastic displacement ratios are not significantly affected by changes in the epicentral distance or the closest distance to the horizontal projection of the rupture (Miranda, 2000; Chopra and Chintanapakdee, 2001, 2004; Ruiz-García and Miranda, 2003, 2004, 2006; Ruiz-García, 2011). However, the effect of earthquake magnitude on the inelastic displacement ratio is more than that of the site to source distance (Akkar and Küçükdoğan, 2008). In general, it can be said that the effects of faulting mechanism, earthquake magnitude and distance to rupture on inelastic displacement ratio are implicitly taken into account when the effects of the other important factors (i.e. T_c, T_g and A_p/V_p) are considered.

Soil condition and site classes

The effects of soil conditions on the inelastic displacement ratio have been studied by many researchers (Miranda, 2000; Chopra and Chintanapakdee, 2001, 2004; Riddell, Garcia and Garces, 2002; Ruiz-García and Miranda, 2003, 2004, 2006; Mollaioli and Bruno, 2008; Durucan and Dicleli, 2015). From the review of these investigations, soil conditions can be categorized into firm soil (NEHRP site classes B, C, and D) and soft soil (NEHRP site classes E and F). For the firm sites, inelastic displacement ratios were not significantly affected by local site conditions (NEHRP site classes B, C, and D), especially for long periods and when the period scale is normalized relative to the T_c value (Miranda, 2000; Chopra and Chintanapakdee, 2001, 2004; Ruiz-García and Miranda, 2003). However, for soft soils, the predominant period of the ground motion, T_g, is important. Dispersion of C is not constant over the whole normalized period range (T/T_g), tending to increase as T/T_g decreases. In general, the record-to-record variability of C is smaller for ground motions recorded on soft soil than for ground motions recorded on rock or firm soil sites (Ruiz-García and Miranda, 2004, 2006).

Response data for 216 ground motions recorded on NEHRP site classes B, C, and D demonstrated that neglecting the effect of site classes for structures with periods smaller than 1.5 s built on firm sites will typically result in errors less than 20% in the estimation of mean inelastic displacement ratios, whereas for periods longer than 1.5 s the errors are smaller than 10%. Differences are even smaller if $R \leq 3$ (Ruiz-García and Miranda, 2003). In general, it can be said that the effects of soil conditions on inelastic displacement ratio are implicitly taken into account when the effects of the other proper factors (i.e. T_c , T_g and A_p/V_p) are considered.

Hysteretic behavior, post-yield stiffness, and structural degradation

Some researchers have concluded that the inelastic displacement ratio in the acceleration-sensitive spectral region is reduced because of post-yield stiffness(Veletsos, 1969; Xiaoxuan and Moehle, 1991; Chopra and Chintanapakdee, 2004), and increased due to stiffness degradation (Xiaoxuan and Moehle, 1991; Song and Pincheira, 2000; Ruiz-García and Miranda, 2004; Chenouda and Ayoub, 2008; Ruiz-García, 2011) and pinching (Gupta and Krawinkler, 2000; Song and Pincheira, 2000) of the hysteresis loop. On the other hand, at longer periods, the influence of post-yield stiffness ratio, α, on the inelastic displacement ratio is not significant (Chopra and Chintanapakdee, 2004; Ruiz-García and Miranda, 2006; Mollaioli and Bruno, 2008; Ruiz-García, 2011) and the mean responses of constant-ductility systems can be conservatively estimated using the elastoplastic model (Riddell, Garcia and Garces, 2002; Ruiz-García and Miranda, 2003, 2004; Ruiz-García, 2011). Chopra and Chintanapakdee (Chopra and Chintanapakdee, 2004) concluded that ignoring post-yield stiffness in estimating deformation is too conservative for seismic evaluation of existing structures with known strength ratio in the acceleration-sensitive region.

An investigation based on 118 ground motion records on soft soils demonstrated that strength and (or) stiffness degradation can result in considerable increments in deformation demands for systems with periods of vibration that are smaller than $0.5T_g$ of the ground motion. However, for systems with T longer than T_g, maximum inelastic displacement demands of degrading systems tend to be smaller than those of non-degrading systems (Ruiz-García and Miranda, 2006). The effects of stiffness degradation are more important on structures built on soft soil than for structures on rock or firm soil sites (Ruiz-García and Miranda, 2004). Form comparison of the results obtained based on 40 forward-directivity near-fault ground motions (Ruiz-García, 2011) with those obtained from a total 216 ordinary far-field ground motions(Ruiz-García and Miranda, 2003), it can be concluded that the effect of post-yielding stiffness in limiting maximum inelastic displacements demands is less beneficial for SDOF systems exposed to forward directivity near-fault ground motions than for systems subjected to far-field ground motions.

Response data for 80 ground motion records (Chenouda and Ayoub, 2008) demonstrated that for short period SDOF systems the inelastic displacement of the degrading systems were substantially larger than the corresponding displacements of non-degraded systems and collapse is typically observed for very short period systems, even for systems with low strength reduction factors (R). However, for long period degrading systems, collapse is not expected, even for systems with large strength ratios and the well-known equal displacement rule is preserved even for these systems. Moreover, since the behavior of peak-oriented models is dominated by accelerated degradation, which strongly increases the inelastic displacements, the effect of degradation on the maximum inelastic displacements is lower for bilinear models than for modified Clough models. Furthermore, bilinear models have a faster collapse rate than peak-oriented models for short period structures. This is due to the fact that bilinear models dissipate the largest hysteretic energy and, hence, reach their capacity earlier (Chenouda and Ayoub, 2008).

Ductility demand and strength ratio

The available relationships for inelastic displacement ratios in the literature can be categorized into two groups. First, the so-called constant-ductility inelastic displacement ratio relationships expressed as a function of elastic vibration period, T, and ductility demand factor, μ, which is very useful in the preliminary design of new or rehabilitated structures where an estimate of the global displacement ductility capacity is known. Second, the so-called constant-strength inelastic displacement ratio relationships expressed as a function of T and strength ratio, R, which can be used to determine the inelastic deformation of an existing structure with known strength. Thus, these two parameters (R and μ) are the important factors that affect the inelastic displacement ratios. It should be noted that the use of constant-ductility inelastic displacement ratios underestimates the expected value of the maximum deformations in systems with known strength ratio (Miranda, 2001; Ruiz-García and Miranda, 2003).

The average values of inelastic displacement ratio greater than one in the acceleration-sensitive spectral region, and increases as the level of ductility demand or strength ratio increases; approximately equal to one in the velocity- and displacement-sensitive regions, essentially independent of μ and R; except for the period range that they fall below unity, decreasing for increasing μ and R (Chopra and Chintanapakdee, 2004; Ruiz-García and Miranda, 2004, 2006). For very short-period systems, inelastic displacement ratio is very sensitive to the yield strength and can be very large even if the strength of the system is only slightly smaller than that required for it to remain elastic (Chopra and Chintanapakdee, 2004).

An Investigation based on 116 ground motion records on soft soils showed that the dispersion on inelastic displacements ratios increases as the level of ductility demand increases (Ruiz-García and Miranda, 2004). Response data for 216 ground motions (Ruiz-García and Miranda, 2003) concluded that dispersion of C is relatively large for R higher than 4 and T smaller than 1.5 s. Limiting periods dividing regions where the equal displacement rule is applicable from those where this rule is not applicable depend primarily on R value and the level of μ. These limiting periods increase with

increasing μ and R (Miranda, 2000; Ruiz-García and Miranda, 2003).

A more recent investigation based on 98 near-fault pulse-type and 306 far-fault ground motion records (Durucan and Dicleli, 2015) showed that for strong earthquakes ($A_p/V_p < 10$) the strength ratio significantly affects the variation of inelastic displacement ratios. However, for weak ($A_p/V_p > 20$) and moderate ($10 < A_p/V_p < 20$) earthquakes, the effect of the strength ratio on the variation of C is small and moderate, respectively. The strength ratio has a great influence on the collapse potential of degrading structures (Chenouda and Ayoub, 2008) and the effect of sequential earthquake loading is more pronounced for the systems with larger R values (Durucan and Durucan, 2016).

MDOF systems considered in this study

To investigate the accuracy of linear dynamic analysis for estimating local inelastic deformation of MDOF System using SDOF inelastic displacement ratio, a total of 8 regular MDOF systems having different natural period of vibrations were selected. These MDOF systems were assembled based on regular two-dimensional moment resisting frame structures. In the other words, the geometry, degree of indeterminacy (or redundancy), and deformation of the MDOF systems were considered to be in accordance with the characteristics of two-dimensional moment resisting frames. Since the vibration period (T) and the strength ratio (R) were the main considered variables in this study, some idealizations were made to prevent the effects of other parameters (i.e. hysteresis behavior, plastic hinge length and so on) on the results. Thus, each MDOF system was assembled from elastoplastic rotational springs and elastic beam-column elements as shown in Fig. 1. In such a system it is possible to directly compare the local deformations (spring rotations) obtained from linear analysis with those obtained from the nonlinear analysis. Each frame had 5 stories with the height of 3.2 m and 3 bays with the width of 5 m. The distance of each rotational spring from its adjacent joint was equal to 5% of the bay length (or story height). All the elements except rotational springs were linear elastic. The elastoplastic (elastic-perfectly plastic) model was used to present the hysteresis behavior of the springs. Since the force distribution between members of a system depends on relative stiffness of each member (and the force redistribution depends on relative plastic strength of each member), the stiffness and plastic strength of the springs for each MDOF system were obtained based on a regular steel moment resisting frame structure designed according to usual design codes. These values are shown in Fig. 1. The mass was concentrated at story levels as a line mass along the story beams. The value of the line mass was calculated to achieve the desired value for the natural period. These MDOF systems were different in the natural period of vibration as shown in Fig. 1. As described in the next section, in this investigation, strength ratio (R) was controlled via the earthquake intensity.

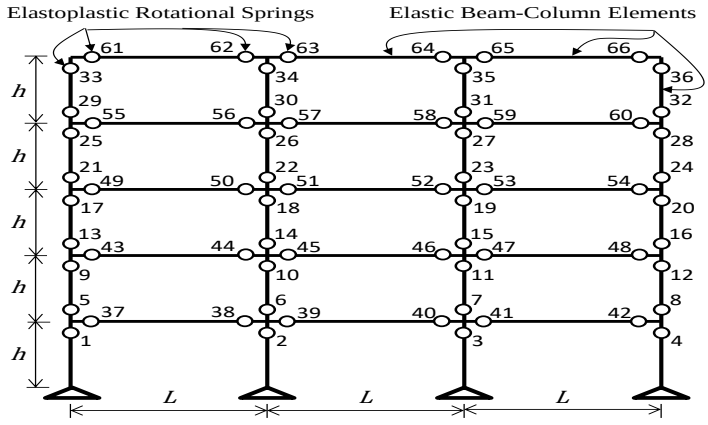

$L = 5.0\ m$
$h = 3.2\ m$

Spring	$K_\theta\ (kN.m)$	$M_p\ (kN.m)$
1 ~ 4	487200	416
5 ~ 12	239164	240
13 ~ 28	124688	155
29 ~ 36	86284	104
37 ~ 42	388584	314
43 ~ 48	273336	245
49 ~ 54	197736	193
55 ~ 60	140381	151
51 ~ 66	97272	116

MDOF Model Name:	F-1	F-2	F-3	F-4	F-5	F-6	F-7	F-8
Line Mass ($kN.S^2/m/m$):	0.285	0.641	1.139	1.779	2.561	3.486	4.553	5.762
Natural Period (S):	0.50	0.75	1.00	1.25	1.50	1.75	2.00	2.25

Fig 1. Configuration and details of the MDOF systems

Table 1: Main properties of the considered ground motions.

Earthquake Name	Year	Station	M	Mechanism	Rjb (km)	Rrup (km)	V_{s30} (m/s)	PEER Seq. #
Superstition Hills-02	1987	El Centro Imp. Co. Cent	6.54	Strike-slip	18.2	18.2	192.05	721
Imperial Valley-06	1979	Delta	6.53	Strike-slip	22.03	22.03	242.05	169
Kobe, Japan	1995	Shin-Osaka	6.9	Strike-slip	19.14	19.15	256	1116
Kocaeli, Turkey	1999	Duzce	7.51	Strike-slip	13.6	15.37	281.86	1158
Loma Prieta	1989	Capitola	6.93	Reverse Oblique	8.65	15.23	288.62	752
Duzce, Turkey	1999	Bolu	7.14	Strike-slip	12.02	12.04	293.57	1602
Northridge-01	1994	LA - Saturn St	6.69	Reverse	21.17	27.01	308.71	1003
San Fernando	1971	LA - Hollywood Stor FF	6.61	Reverse	22.77	22.77	316.46	68
Superstition Hills-02	1987	Poe Road (Temp)	6.54	Strike-slip	11.16	11.16	316.64	725
Landers	1992	Joshua Tree	7.28	Strike-slip	11.03	11.03	379.32	864
Chi-Chi, Taiwan	1999	TCU095	7.62	Reverse Oblique	45.15	45.18	446.63	1524
Friuli, Italy-01	1976	Tolmezzo	6.5	Reverse	14.97	15.82	505.23	125
Northridge-01	1994	Beverly Hills - 12520	6.69	Reverse	12.39	18.36	545.66	952
Manjil, Iran	1990	Abbar	7.37	Strike-slip	12.55	12.55	723.95	1633
Hector Mine	1999	Hector	7.13	Strike-slip	10.35	11.66	726	1787

Rjb: Joyner-Boore distance to rupture plane
Rrup: Closest distance to rupture plane

Earthquake ground motions

The set of 15 ground motion records used in this investigation are listed in Table 1. These far-field records were selected from the strong ground motion database of the Pacific Earthquake Engineering Research (PEER) Centre (http://ngawest2.berkeley.edu/site). These records had been also used by FEMA p695 (ATC-63 Project) (ATC, 2009).

To ensure that each MDOF system responds into different inelastic range (nearly elastic, medium and high strength ratio) when subjected to ground motions, each record was scaled to three PGA for the MDOF system. Records with smaller PGA (L-PGA) were used to produce low demand ductility (nearly elastic - $R \cong 2$) in the system; Records with intermediate PGA (M-PGA) were used to produce medium demand ductility in the system ($R \cong 3.5$), while records with greater PGA (H-PGA) were used to produce high demand ductility in the system ($R \cong 5$). It should be mentioned that for each earthquake record, the L-PGA, M-PGA and H-PGA vary for different MDOF systems.

Accuracy evaluation procedure

In this investigation, the roof displacement was considered as the global deformation while the rotations of the springs were considered as the local deformations. Approximate roof displacement for each MDOF system subjected to each ground motion record was calculated as the product of the maximum roof displacement obtained from the linear dynamic analysis times the inelastic displacement ratio obtained from an equivalent SDOF system subjected to the ground motion record. The period and the strength ratio of the equivalent SDOF system were the same as those of the MDOF system. However, for each spring of the MDOF system, two approximate rotations were calculated. The first one ($\theta_{ap.i}$) was calculated based on the inelastic displacement ratio obtained for the roof displacement of the MDOF system. The second one ($\theta^*_{ap.i}$) was computed based on the inelastic displacement ratio obtained from a new SDOF system with the strength ratio equal to the strength ratio of the spring and with the period equal to the period of the MDOF system. In summary, the accuracy of linear dynamic analysis for estimating global and local inelastic deformations of MDOF Systems using SDOF inelastic displacement ratios was evaluated using the following steps:

1- Perform a nonlinear static analysis (pushover) for each MDOF system to generate the capacity carve of the system and to calculate the capacity base shear of the system (V_y).

2- Perform a linear time history analysis (LTHA) for the MDOF system subjected to each ground motion record to calculate the L-PGA, M-PGA, and H-PGA of the ground motion record for the MDOF system as the following sub-steps:

a. Using the maximum elastic base shear (V_E) obtained from the LTHA and V_y, compute the initial strength ratio as $R_0 = V_E/V_y$,

b. For the desired strength ratio values corresponding to the Low-, Medium- and the high-strength ratio (i.e. R_1, R_2 and R_3,

respectively), calculate the corresponding ground motion scale factors as $SF_i = R_i/R_0$ ($i = 1, 2$ and 3).

3- Compute the elastic global deformation (roof displacement), Δ_E, and the elastic local deformations (spring rotations), θ_{Ei}, of the MDOF system subjected to the ground motion record with different intensities (L-PGA, M-PGA, and H-PGA). These deformations can be calculated by multiplying the deformations obtained from LTHA of Step 2 by the corresponding SF_i calculated from Step 2-a.

4- For each spring of the MDOF system subjected to the ground motion record with the specific intensity (L-PGA, M-PGA or H-PGA) calculate the local strength ratios as $R_L = M_E/M_y$, in which M_E and M_y are the maximum earthquake-induced bending moment obtained from LTHA (by considering SF_i) and the bending capacity of the spring, respectively.

5- For each spring of the MDOF system subjected to the ground motion with the specific intensity, if $R_L \leq 1$ then the corresponding SDOF inelastic displacement ratio $C_L = 1$, else (i.e. if $R_L > 1$) compute C_L as the following sub-steps:

a. Generate an SDOF system with the period of vibration equal to the period of vibration of the MDOF system.
b. Perform LTHA for the SDOF system subjected to the ground motion record to obtain the elastic displacement (δ_E) and the elastic force (f_E).
c. Calculate the plastic strength of the SDOF system for strength ratio equal to R_L as $f_y = f_E/R_L$.
d. Perform a nonlinear time history analysis (NTHA) for the SDOF system subjected to the ground motion record to obtain the inelastic displacement (δ_{in}).
e. Compute the inelastic displacement ratio as $C_L = \delta_{in}/\delta_E$.

6- For each spring of the MDOF system subjected to the ground motion with the specific intensity compute the approximate inelastic rotation of the spring as $\theta^*_{ap.i} = C_L\theta_{Ei}$.

7- For the MDOF system subjected to the ground motion with the specific intensity, compute the inelastic displacement ratio (C) using a SDOF system with the period of vibration equal to the period of vibration of the MDOF system and the strength ratio equal to the corresponding R_i (R_1, R_2 or R_3). The sub-steps are similar to the Step 5-sub-steps.

8- Calculate the approximate inelastic roof displacement of the MDOF system as $\Delta_{ap} = C\Delta_E$.

9- Calculate another approximate inelastic rotation for each spring as $\theta_{ap.i} = C\theta_{Ei}$.

10- Perform NTHA for the MDOF system subjected to the ground motion record with the specific intensity to obtain the exact inelastic roof displacement (Δ_{ex}) and the exact inelastic rotation of the springs ($\theta_{ex.i}$).

11- Compute the error indices as defined in the next section for the local (spring rotations) and global (roof displacement) deformations. These indices were computed for all combinations of the ground motions, the period of vibrations, and the strength ratio levels.

12- For each period of vibration and each level of strength ratio, calculate median, average and cumulative percentage of the error indices for statistical interpretation and discussion.

13- Compare the error index values for local and global deformations.

Correlation factor and error indices

Correlation analysis is one of the practical methods which can be used for estimating the accuracy of an analysis method. In this research, the Pearson product-moment correlation coefficient, ρ, is used. The coefficient is computed as follows:

$$\rho = \frac{\sum_{i=1}^{m}\left(Q_i^N - \overline{Q^N}\right)\left(Q_i^L - \overline{Q^L}\right)}{\sqrt{\sum_{i=1}^{m}\left(Q_i^N - \overline{Q^N}\right)^2} \times \sqrt{\sum_{i=1}^{m}\left(Q_i^L - \overline{Q^L}\right)}} \quad (1)$$

Where m is the total number of data. Q_i^N is the NTHA response (such as roof displacement and rotation of springs) for the i^{th} ground motion and Q_i^L is the corresponding estimated response from the approximate LTHA for the i^{th} ground motion. $\overline{Q^N}$ is the average of m NTHA results, and $\overline{Q^L}$ is the average of m approximate LTHA results. This coefficient is the measurement of correlation and ranges between $+1$ and -1. $\rho = 0$ indicates no relationship between the two measures, $\rho = +1$ indicates the strongest positive correlation possible, and $\rho = -1$

indicates the strongest negative correlation possible.

The well-known relative error index is also used in this research which is calculated as follows:

$$Err_i(\%) = \frac{Q_i^L - Q_i^N}{Q_i^N} \times 100 \qquad (2)$$

If the relative error index values are positive, the approximate LTHA procedure overestimates response and vice versa. Another practical measure for estimating the accuracy of the approximate LTHA is the root mean square error, which can be calculated by the following equation:

$$Err_{RMS}\ (\%) = \sqrt{\frac{1}{m}\sum_{i=1}^{m}\left(\frac{Q_i^L - Q_i^N}{Q_i^N}\right)^2} \times 100 \qquad (3)$$

This error index represents the sample standard deviation of the differences between predicted values and actual values.

Statistical results for global responses

The conservatism and accuracy of the LTHA for estimating roof displacement can be presented by scatter plotting the roof displacements estimated by the LTHA versus the roof displacements resulted from the NTHA as shown in Fig. 2.

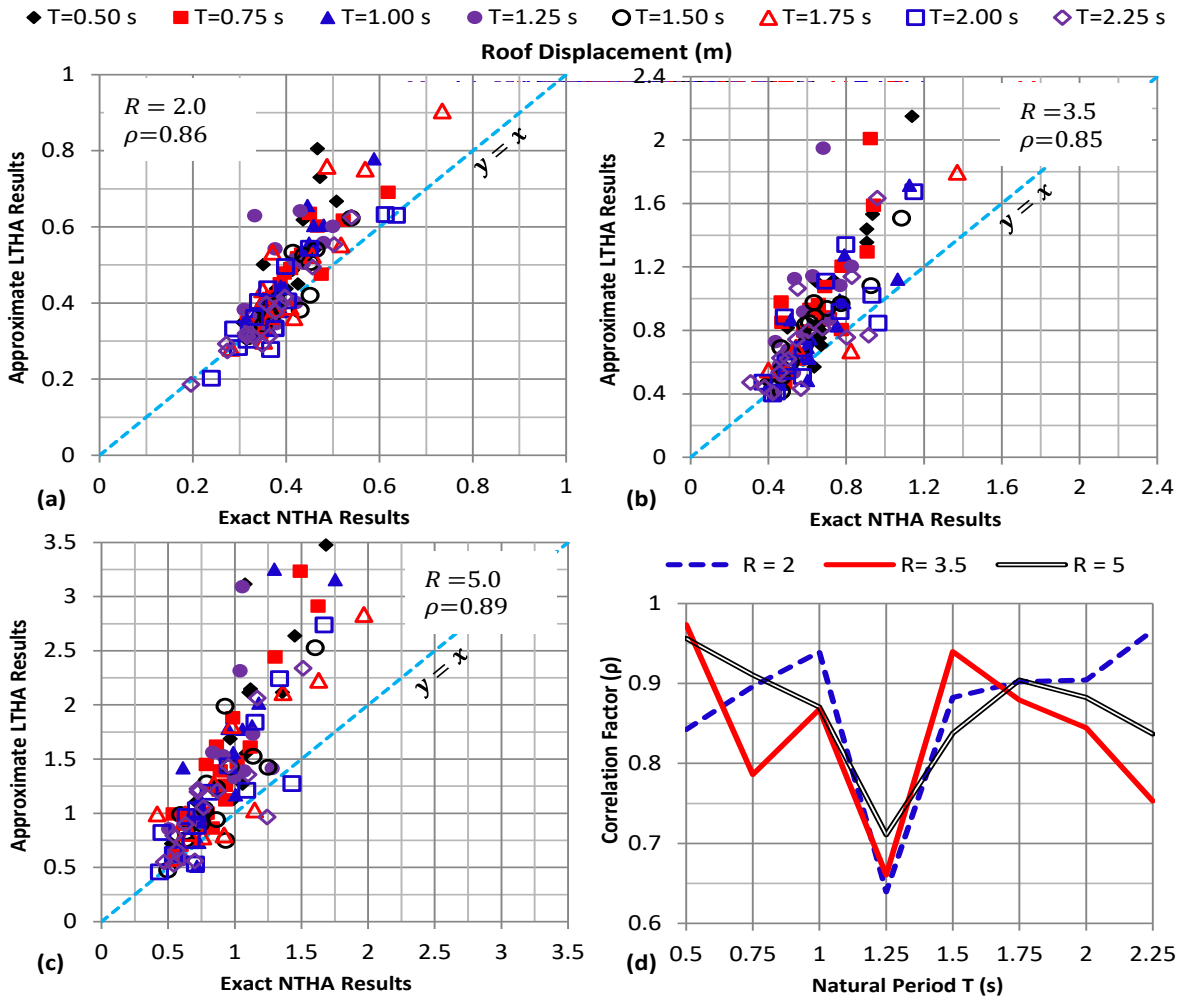

Fig 2. Scatter plots of the roof displacements estimated by the LTHA versus those resulted from NTHA

Each graph of Fig. 2a to Fig. 2c has been plotted for $m = 8 \times 15 = 120$ data points. In these graphs, if the data points are located above the line $y = x$, indicating that the LTHA overestimates roof displacements and vice versa. It can be seen that the tendency of the LTHA to overestimate roof displacement increases with the decrease of the natural period of vibration or with the increase of ductility demand of structures. In general, the LTHA overestimated the roof displacement for about 82% of the cases. For all data points, the

correlation factor is 0.92 showing good correlation between the estimated roof displacements and those obtained from the nonlinear time history analysis (individual correlation factor for each MDOF system and each strength ratio is presented in Fig. 2d).

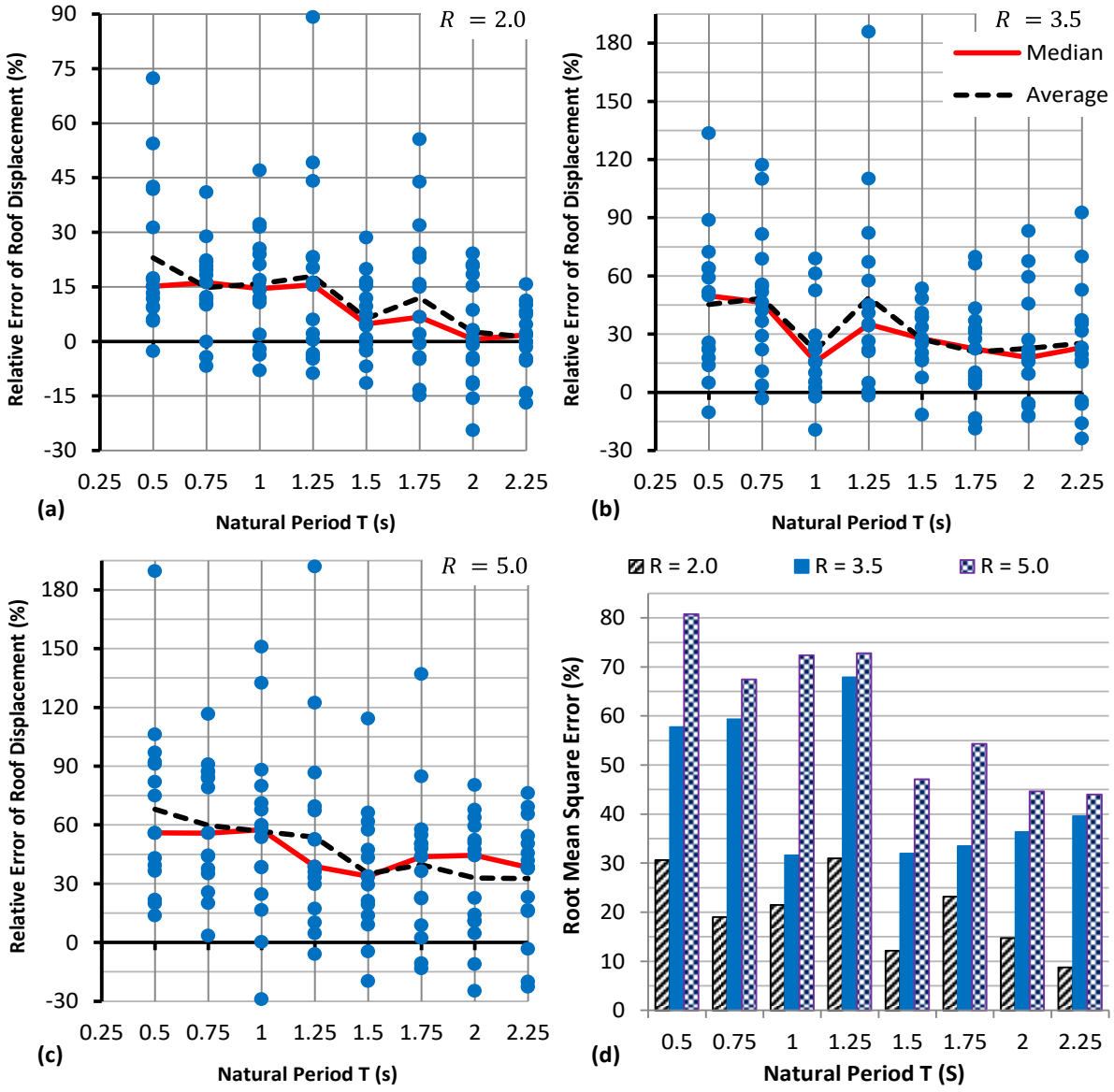

Fig 3. Relative and root mean square errors of the roof displacements estimated by the LTHA Procedure

The relative error distribution of the estimated roof displacement for MDOF systems with different natural period and different strength ratio are shown in Fig. 3a through Fig. 3c. In these graphs, each point corresponds to an MDOF system subjected to a specific earthquake record. The average of the data is shown by the solid line while the dashed line is used to represent the median of the data. It can be seen that the relative error decreases as the natural period of vibration increases. However, by increasing strength ratio the relative error also increases. It can be said that the relative error value for estimating roof displacement via LTHA is on average about 30% on the safe side. Fig. 3d illustrates the root mean square errors of the estimated maximum roof displacements for MDOF systems with different natural period and different strength ratio.

Statistical results for local responses

Fig. 4 illustrates the scatter plots of the spring rotations estimated by different linear dynamic analysis procedure versus spring rotations obtained from the nonlinear time history analyses.

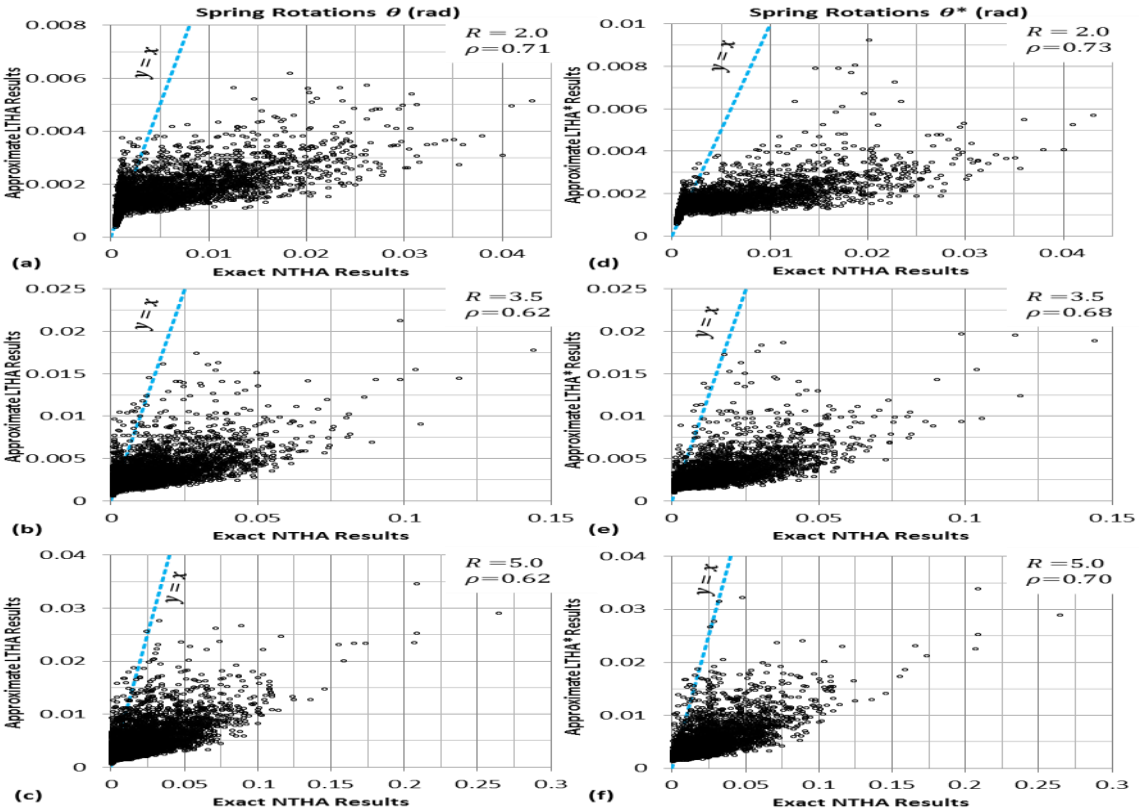

Fig 4. Scatter plots of the spring rotations estimated by the LTHA versus those resulted from NTHA.

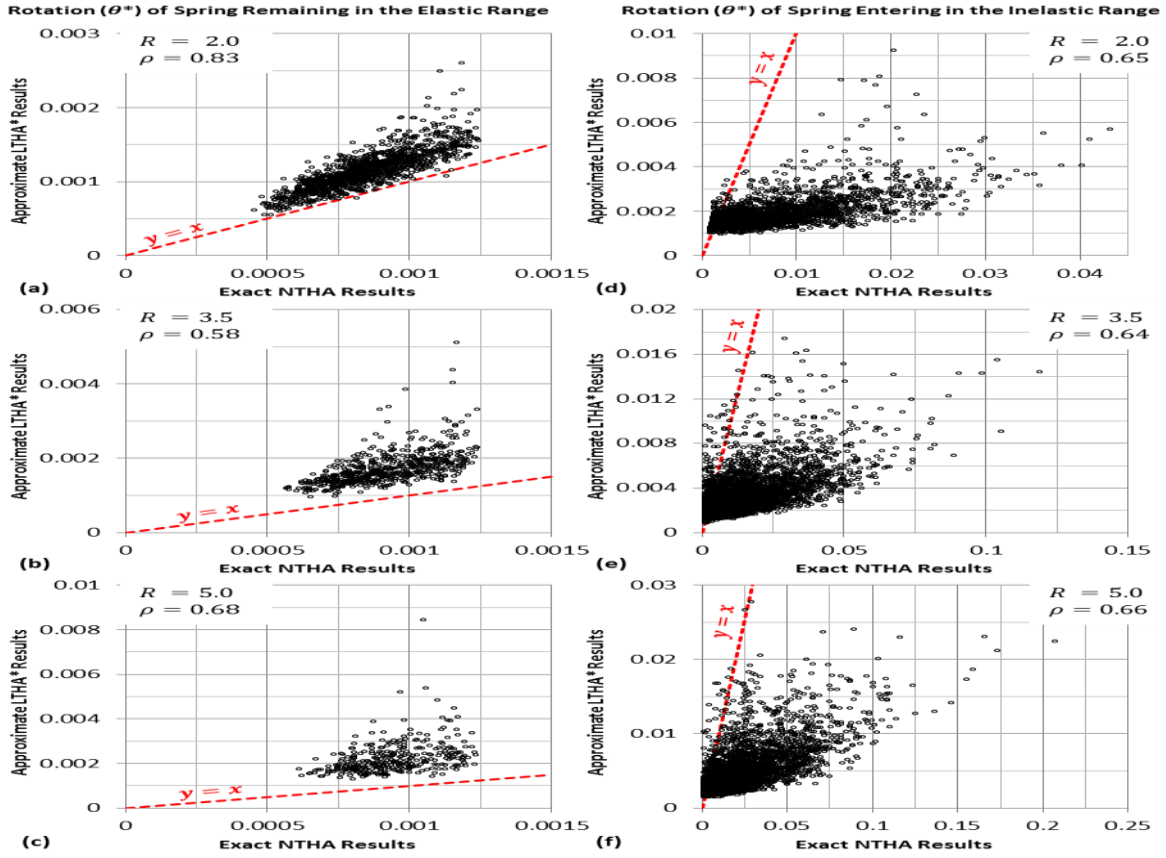

Fig 5. Scatter plots of the spring rotations estimated by the LTHA versus those resulted from NTHA: (a), (b) and (c) for springs remaining in the elastic range, (d), (e) and (f) for springs entering in the inelastic range

One of the approximate procedures used the inelastic displacement ratio obtained for the roof displacement of the MDOF system (Fig. 4a through Fig. 4c); while the second one used the inelastic displacement ratio obtained from a new SDOF system with the strength ratio equal to the strength ratio of the spring and with the period equal to the period of the MDOF system (Fig. 4d through Fig. 4f). Each graph of Fig. 4 has been plotted for $m = 8 \times 15 \times 66 = 7920$ data points. It is clear from these graphs that both approximate procedures tend to underestimate the spring rotations for many cases. In general, the LTHA procedures underestimated the spring rotations for about 75% of the cases. For all data points, the correlation factors for the first and the second LTHA procedures are 0.70 and 0.74, respectively (individual correlation factor for each strength ratio is presented in Fig. 4). It is important to note that the LTHA procedures overestimate the rotation of springs which remain in the elastic range and tend to underestimate the rotation of springs that entering the inelastic range. This issue is shown in Fig. 5 in which the scatter plots are drawn individually for the springs which remained in the elastic range and the springs that entered in the inelastic range.

The relative error distribution of the spring rotations for MDOF systems with different natural period and different strength ratio are shown in Fig. 6. In this figure, the left graphs are related to the LTHA procedure which used the inelastic displacement ratio obtained for the roof displacement of the MDOF system while the right graphs are related to the LTHA procedure that used the inelastic displacement ratio obtained from a new SDOF system with the strength ratio equal to the strength ratio of the spring and with the period equal to the period of the MDOF system. In these graphs, each point corresponds to a spring of an MDOF system subjected to a specific earthquake record. The average of the data is shown by the solid line while the dashed line is used to represent the median of the data. It can be seen that the relative errors for spring rotation obtained from the second LTHA procedure (θ^*) are less than those obtained from the first LTHA procedure (θ). However, by increasing strength ratio the relative error increases. It can be said that the relative error value for estimating spring rotation via LTHA is on average about 35% on the unsafe side. Nevertheless, it is important to realize that dispersion of the relative errors in some cases is substantial, particularly for large levels of inelastic behavior. Thus, when applied to individual ground motion records; the LTHA methods could lead to significant errors in the estimation of local deformation. Fig. 7 illustrates the root mean square errors of the estimated spring rotations for MDOF systems with different natural period and different strength ratio.

The dispersion of the relative errors of spring rotations for two LTHA procedures is explained in Fig. 8. In this figure, the vertical axis of each graph represents the percentage of the springs whose relative errors are higher than those values shown on the horizontal axis of the graph. For each strength ratio (R), two curves are provided. The first curve is presented for the relative error percentage on the safe side and the second curve is developed for the relative error percentage on the unsafe side. For example, in Fig. 8b, it can be observed that, for $R = 3.5$, the spring rotations are underestimated at least by 20% for about 75% of springs and are overestimated at least by 60% for about 15% of springs. This means that for about 10% of the potential plastic hinges, the relative errors of the spring rotations are between -20% and +60%.

Comparison of local and global responses

From the presented results in the previous sections, it is clearly evident that the accuracy of the approximate linear dynamic analysis procedures for estimating local deformations is less than the accuracy of these methods for estimating global deformations. By comparing Fig. 2 and Fig. 4, it can be seen that there is a good correlation between the estimated global deformation and those obtained from the nonlinear time history analysis while for the local responses the correlation is not well. The relative error values for global responses vary between -30% to +180% while these values for local responses vary between -100% to 1200% or between -100% to 750% for the first and second LTHA procedures, respectively. And most importantly, on average, the LTHA overestimates global deformations while this approximate method underestimates local deformations. Dispersion is relatively very high for local responses. Summary of the results is presented in Table 2.

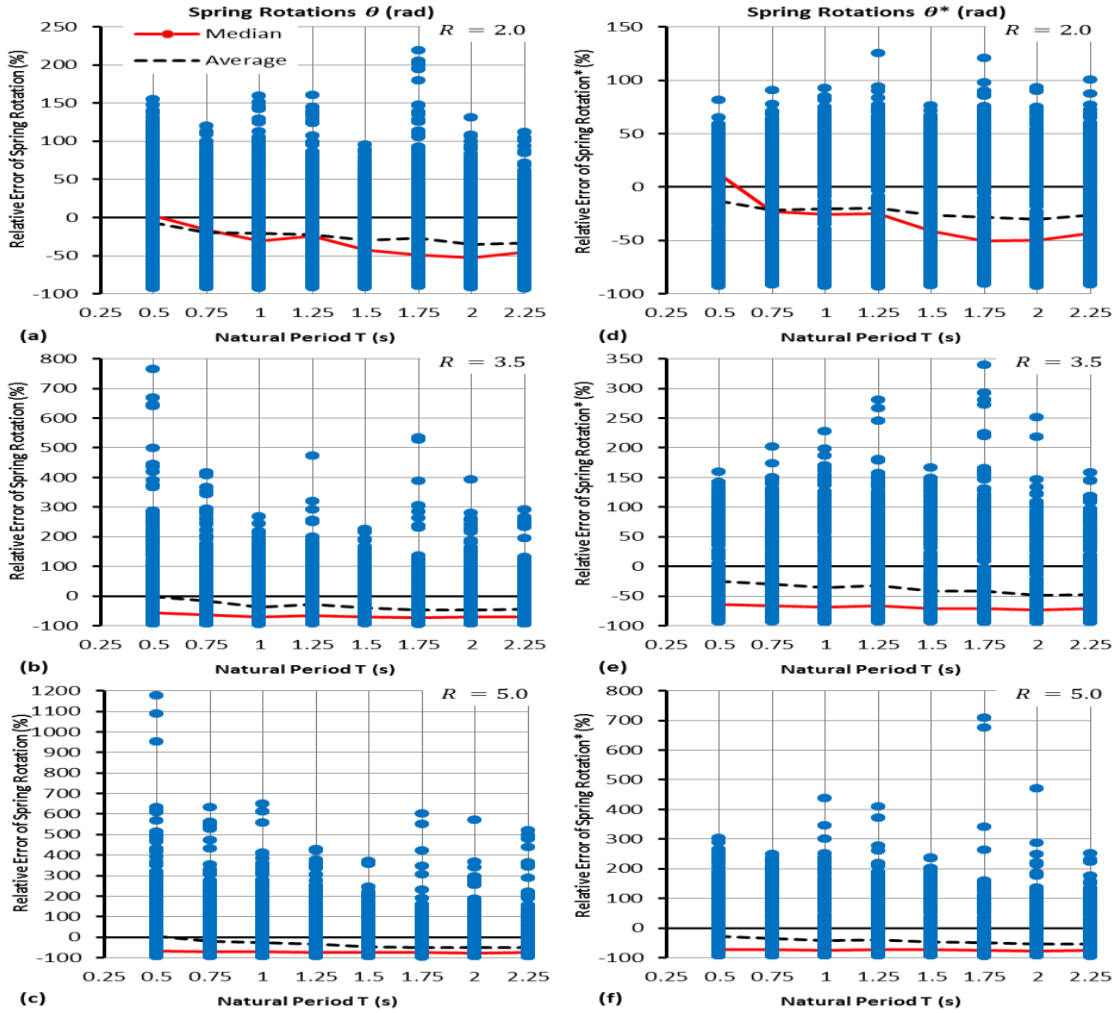

Fig 6. Relative errors of the spring rotations estimated by the LTHA Procedures

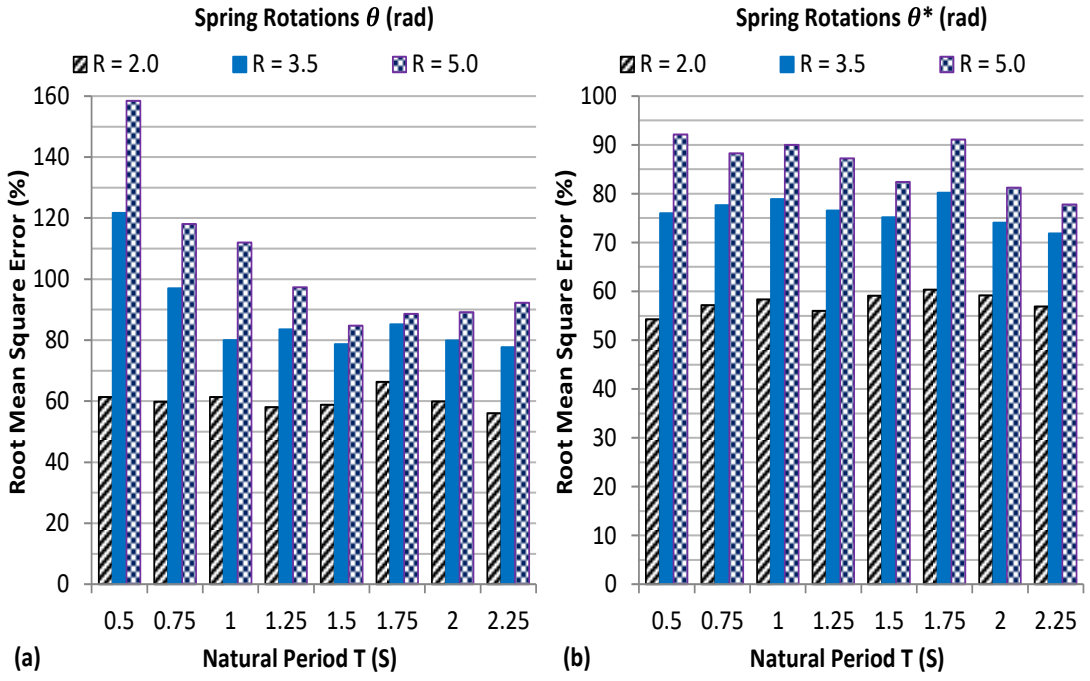

Fig 7. Root mean square errors of the spring rotations estimated by the LTHA Procedures.

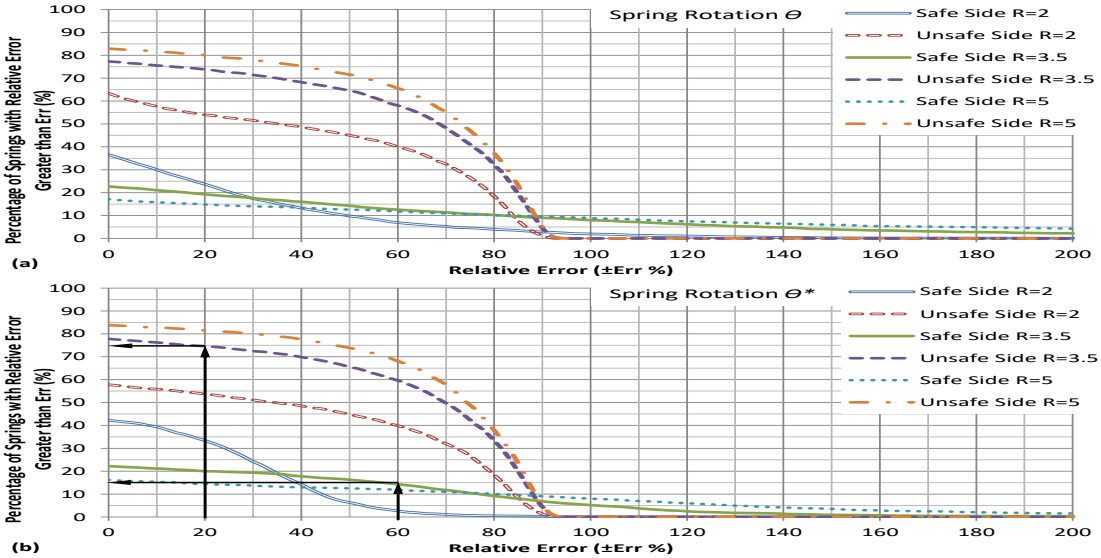

Fig 8. Dispersion of the relative errors of spring rotations

Table 2: Summary of the results obtained for global and local responses.

	Global Deformations					
	$R = 2$		$R = 3.5$		$R = 5$	
Correlation factor (ρ)	0.86		0.85		0.89	
Variation of median of Err	0.6 ~ 16.2		15.8 ~ 49.8		33.8~57.6	
Median of Err for all data	10.03		26.00		44.23	
Variation of RMS errors	8.8 ~ 31.1		31.6 ~ 67.9		44.1 ~ 80.8	
RMS error for all data	21.56		46.75		61.98	
	Local Deformations (θ and θ^*)					
	$R = 2$		$R = 3.5$		$R = 5$	
Correlation factor (ρ)	0.71	0.73*	0.62	0.68*	0.62	0.67*
Variation of median of Err	-53 ~ 2	-50 ~ 12*	-73 ~ -57	-73 ~ -64*	-76 ~ -67	-76 ~ -73*
Median of Err for all data	-35.47	-34.37*	-68.71	-69.72*	73.30	-74.47*
Variation of RMS errors	56 ~ 66	54 ~ 60*	78 ~ 122	72 ~ 80*	85 ~ 159	78 ~ 92*
RMS error for all data	60.32	57.70*	89.06	76.34*	107.59	86.42*

Summary and conclusions

The displacement coefficient method is widely used by the profession to estimate seismic deformation demands of structures. Although this method has been the topic of several investigations over the last two decades the vast majority of these investigations are related to the estimation of roof inelastic displacement demands (global deformations) of structures; and there is a lack of evidence about the ability of the method to estimate local deformations of structures. This paper investigated the accuracy of linear dynamic analysis for estimating local deformations of regular MDOF systems using SDOF inelastic displacement ratio. To attain this objective, 8 regular MDOF systems with different natural period of vibration subjected to 15 ground motion records were selected. To ensure that each MDOF system responds into different inelastic range when subjected to ground motions, each record was scaled to three PGA for the MDOF system. For each spring of the MDOF systems, two approximate rotations were calculated. The first one ($\theta_{ap.i}$) was calculated based on the inelastic displacement ratio obtained for the roof displacement of the MDOF system. The second one ($\theta^*_{ap.i}$) was computed based on the inelastic displacement ratio obtained from a new SDOF system with the strength ratio equal to the strength ratio of the spring and with the period equal to the period of the MDOF system. This investigation has led to the following conclusions:

1- There is a good correlation between the global deformations obtained from the approximate linear dynamic analysis and those obtained from the nonlinear time history analysis. However, the correlation

between the local deformations obtained from the approximate linear dynamic analysis procedures and those obtained from the nonlinear time history analysis is not suitable.

2- In general, the relative errors for estimating local deformations are very larger than those for estimating global deformations. The dispersion is also relatively very high for local responses.

3- Based on the median values, the approximate linear dynamic analysis procedure overestimates global deformations while this approximate method underestimates local deformations.

4- It should be noted that the approximate linear dynamic analysis procedures overestimate the local deformations which remain in the elastic range and tend to underestimate the local deformations that entering in the inelastic range.

5- The results presented in this study indicate that although the inelastic displacement ratio obtained from SDOF systems provides an acceptable estimation of the global response of MDOF systems, it is not suitable for estimating the local responses of the MDOF systems.

Abbreviations

ATC	Applied Technology Council
FEMA	Federal Emergency Agency Management
LTHA	Linear Time History Analysis
MDOF	Multi Degree of Freedom
NTHA	Nonlinear Time History Analysis
PEER	Pacific Earthquake Engineering Research
PGA	Peak Ground Acceleration
SDOF	Single Degree of Freedom

Nomenclature

A_p	Peak ground acceleration
C	Inelastic displacement ratio
C_L	Inelastic displacement ratio for local deformation
Err_i	Relative error index
Err_{RMS}	Root mean square error
f_E	Elastic force of the SDOF system obtained from LTHA
f_y	Plastic strength of the SDOF system
M_E	Maximum earthquake-induced bending moment obtained from LTHA
M_y	Bending capacity (plastic moment) of the spring
Q_i^L	Estimated response from the approximate linear dynamic analysis for the i^{th} ground motion
$\overline{Q^L}$	Average of the estimated linear dynamic analysis results
Q_i^N	Nonlinear time history response for the i^{th} ground motion
$\overline{Q^N}$	Average of the nonlinear time history results
R	Strength ratio, defined as the strength required to maintain the system elastic divided by the yield strength
R_i	$i = 0, 1, 2$ and 3 are the initial, low, medium and high strength ratios, respectively
R_L	Local strength ratio, defined as the strength required to maintain the member elastic divided by the capacity strength of the member
SF_i	$i = 1, 2$ and 3 are the ground motion scale factors corresponding to L-, M- and H-PGA, respectively
T	Natural period of vibration of the system
T_c	Characteristic period or corner period, divides the constant acceleration spectral region from the constant velocity spectral region
T_g	Predominant period of the ground motion, defined as the period corresponding to the maximum ordinate in the relative velocity spectrum computed for an elastic SDOF system having 5% damping ratio
T_p	Pulse period of the ground motion, defined as the period associated to the main pulse in the ground velocity time history
V_E	Maximum elastic base shear obtained from the LTHA
V_p	Peak ground velocity
V_y	Capacity base shear obtained from the pushover analysis
α	Post-yield stiffness ratio
Δ_{ap}	Approximate inelastic roof displacement of the MDOF system
Δ_E	Elastic roof displacement of the MDOF system obtained from LTHA
Δ_{ex}	Exact inelastic roof displacement of the MDOF system obtained from NTHA
δ_E	Elastic displacement of the SDOF system obtained from LTHA
δ_{in}	Inelastic displacement of the SDOF system obtained from NTHA
$\theta_{ap.i}$	Approximate inelastic rotation of the ith spring of the MDOF system (based on C)
$\theta^*_{ap.i}$	Approximate inelastic rotation of the ith spring of the MDOF system (based on C_L)
θ_{Ei}	Elastic rotation of the ith spring of the MDOF system obtained from LTHA
$\theta_{ex.i}$	Exact inelastic rotation of the ith spring of the MDOF system obtained from NTHA
μ	Demand ductility of the system
ρ	Pearson product-moment correlation coefficient

References

Abazari, Y & Chavoshian, H. (2002). From Social Class to Lifestyle: New Approaches in the Sociological Analysis of Social Identity, Journal of Social Sciences, No. 20: 27-3.

Adler, a (1956). the individual psychology of alfred adler, newyork: basic books inc. american heriage Dic

Ali, Rahmani Firouzjah et al. (2020). the article titled "Investigation of the effect of household lifestyle on water consumption in Sari city"; The 4th technology development forum and international conference on new findings of civil architecture and construction industry of Iran (Ircivil2019).

Alizadeh, A & Keshavarzi, A. (2005). Status of Agricultural Water Use in Iran, In Water Consumption, Reuse and Recycling; Proceeding of an Iranian- American Workshop: National Academies Press. Http://www. Nap. edu/ catalog/ 11241.htmi

Allender JA, Spradley BW. Community Health Nursing Concepts and Practice. 5th ed. Philadelphia: Lippincott Co, Williams & Wilkins Co; 2001, 314-21

Beheshti, S. (2013). Sociological explanation of consumption of energy carriers and presentation of optimal consumption model, Master's thesis, University of Isfahan.

Bin, Shui; Dowlatabadib, Hadi (2005). Consumer lifestyle approach to US energy use and the related CO2 emissions, Volume 33, Issue 2, Pages 197–208

Burdreu, Pierre, Distinction : A social critique of the Judgment of taste . Routledge, 1984

Chaney, D. (2011). Lifestyle. Translated by Hassan Chavoshian, Tehran: Ministry of Culture and Islamic Guidance, General Directorate of the Secretariat of the Public Culture Council.

David, E. (2005). The Question Environment, London and New York: Routledge

Dolatshahi Pirouz, M. & Tahmasebi Ashtiani, H. (2010), Man, Energy, Environment and Future Vision, Strategy Quarterly, Year 19, Number 56: 313-343.

Fazeli, M. (2009). consumption and lifestyle, Sobh Sadegh Publications, first edition.

Fazeli, M. (2008). A picture of the cultural lifestyle of the student community. Iranian Cultural Research Quarterly, Specially on Lifestyle, Research Institute of Cultural and Social Studies, Ministry of Science, Research and Technology, Tehran: 1 (1), 175-198

Florence, P.V. and A. Jolibert, (1990), "Social values, A.I.O. and consumption patterns" Journal of Business Research Vol 20

Giddens, A. (2011). Modernity and Individuality, translated by Nasser Moafaqian, Tehran: Nei Publishing.

Hashimoto R. Current status, a future trend in fresh water management. International Review for Environmental Strategies, Sustainable Fresh Water Resource Management. 2002; 3 (2): 222-39.

Henryson, J., Hakansson, T. & Pyrko, J. (2000). Energy efficiency in buildings through information – Swedish perspective. Energy Policy, (28): 169-180

Iran Work News Agency, 2-31-2011: http://kargarnews.ir/fa/pages/?cid=8536

IRNA news agency, 21-3-2015: http://www7.irna.ir/fa/News/81662512/

IRNA news agency, news agency of the Islamic Republic of Iran, 8-19-2014: http://www7.irna.ir/fa/News/81833434/

Jabal Ameli, F. & Goudarzi Farahani, Y. (2015). The effect of subsidy reform on the consumption of energy carriers in Iran: a case study of gasoline, oil and diesel consumption, Majles and Strategy, Volume 22, Number 81: 69-89.

Jalaeipour, H. (2013). Late Sociological Theories, Tehran: Ney Publishing.

Kajbaf, M.B., Sajjadian, P & Kaviani, M. (2011), the relationship between Islamic lifestyle and happiness in the life satisfaction of Isfahan students, Psychology and Religion, year 4, number 4: 61-74.

Khani, M.R & Yaghmaian, K. (2002). water purification, Tehran: Dibagaran Cultural and Art Institute.

Kuruvilla, S. J., Nishank, J. And Nidhi, S. (2009). “Do men and women really shop differently? An exploration of gender differences”in mall shopping in India. International Journal of Consumer Studies. 33(6): 715-723

Mahdavi Kani, M.S. (2008). The concept of lifestyle. Quarterly journal of Iranian cultural research, especially lifestyle. Research Institute of Cultural and Social Studies, Ministry of Science, Research and Technology, Tehran: Year 1 (1), 199-230.

Majdi, A.A, Sadr Nabavi, R., Behrwan, H., Houshmand, M. (2010). The lifestyle of young people living in the city of Mashhad and its relationship with the cultural and economic capital of parents, Journal of Social Sciences, Faculty of Literature and Humanities, Ferdowsi University of Mashhad, Paizi and winter.

Mohammadi, A. (2011). study of household electricity consumption among residents of urban areas (case study of Gorgan city), master's thesis, Mazandaran University.

Mohammadi, A., Salehi, S & Khoshfar, G. (2011). lifestyle and its impact on energy consumption, the first international conference on new approaches in energy conservation.

Mohammadpour Lima, H., Poursheykhian, A & Azimi, R. (2011). investigating the relationship between lifestyle and consumption culture and consumerism, Social Sciences, 7th year, number 28:

Palumets, L. (2002). Space of lifestyles in Estonia in 1991. Potsdam: pro ethnologia.

Sanquist, T.F., Orr, H., Shoi, B & Bittner, A.C. (2012). Lifestyle factors in U.S. residential electricity consumption, Volume 42, March, Pages 354–364

Shahabi, M. (2007). Cosmopolitan lifestyles among Iranian youth and its political implications. Collection of Iranian lifestyle patterns. Tehran: Publications of the Research Institute of Strategic Research of the Expediency Council.

Shahnoushi, M & Taji, M.R. (2012). The effect of social networks on the lifestyle of the youth of Shahrekord city, National Studies, Volume 13, Number 51.

Shanesin, M & Rashidkhani, B. (2011). reporting energy consumption and its relationship with weight status and lifestyle in Tehran women aged 18-45, Journal of Endocrinology and Metabolism, Volume 13, Number 2: 156-146.

Simmel, G. (1990). The Philosophy of Money. Tom Bohomer and David Frisby (Trans), second enlarged Ed, New York: Routledge

Thyra, C. (1996). "Definition of Life Style and its Application to Travel Behavior", Department of Marketing at the Aarhus V, Denmark

Yan, S. & Lifang, F. (2011). Influence of psychological, family and contextual factors on residential energy use behaviour: An empirical study of China. Energy Procedia, (5): 910–915.

Zareh Shahabadi, A., Hajizadeh, M & Lotfian, A.M. (2013). Studying the effect of socio-cultural factors on the pattern of energy consumption in households in Yazd city, Planning Research and Energy Consumption Policy, second year, number 3: 17-50.

Zareh, B. & Fallah, M. (2012). Studying the lifestyle of young people in Tehran and the factors affecting it, Cultural Research Quarterly, Volume 5, Number 4, 75-105.